

NEUTRINO MASS FROM COSMOLOGY

GRAZIANO ROSSI

Department of Physics and Astronomy, Sejong University, Seoul, 143-747, Korea

Determining the absolute neutrino mass scale and the number of effective neutrino species are central goals in modern cosmology, at the interface between astrophysics and particle physics. With current or planned large-volume cosmological surveys, these goals are within reach – as data are progressively attaining exquisite quality and high statistical significance. To this end, among different large-scale structure tracers, the Lyman- α forest is re-emerging as a unique tool to probe the neutrino mass at high-redshift – through characteristic imprints on the transmitted Lyman- α flux. We present here a detailed numerical modeling of the low-density regions of the intergalactic medium in presence of massive neutrinos via high-resolution hydrodynamical simulations, and a novel technique to constrain neutrino masses, cosmological parameters, and the number of effective neutrino species from cosmological probes. In particular, we obtain one of the tightest upper bounds on the total neutrino mass ($\sum m_\nu < 0.12$ eV at 95% CL), along with a competitive bound on the number of effective neutrino species ($N_{\text{eff}} = 2.88 \pm 0.20$ at 95% CL). Our results rule out a possible thermalized sterile neutrino at a significance of over 5σ , and provide strong evidence for the cosmic neutrino background ($N_{\text{eff}} = 0$ is rejected at more than 14σ). We also highlight the implications and synergy of our findings with particle physics experiments, and discuss future prospects in neutrino science from cosmology – in view of upcoming large-volume surveys such as DESI, 4MOST, or Euclid.

1 Cosmology and Massive Neutrinos

The renewed interest in neutrino science from cosmology, mainly related to the breakthrough findings from oscillation experiments that neutrinos are massive, has recently drawn increased attention after the well-deserved 2015 Nobel Prize in Physics and the 2016 Breakthrough Prize in Fundamental Physics for the remarkable discovery. The fact that neutrinos are massive particles points at physics beyond the standard scenario.^{1,2} Yet, the nature of massive neutrinos, their absolute mass scale and hierarchy are unknown, as well as the intriguing possibility of additional sterile neutrino components or extra dark radiation degrees of freedom – aside from the three-neutrino standard model.³ To this end, cosmology is becoming progressively competitive in determining the basic properties of neutrinos, by exploiting their characteristic imprints on structure formation due to the neutrino free-streaming and high thermal velocities. It is already feasible to obtain stringent upper bounds on the total neutrino mass $\sum m_\nu$ by combining several cosmological tracers with unrelated systematics, via the impact of massive neutrinos on the large-scale structure (LSS) of the Universe.^{4,5,6,7,8,9} If $\sum m_\nu < 0.1$ eV, a value within reach with planned near-term cosmological surveys such as eBOSS or DESI,^{10,11} one could in principle exclude the inverted hierarchy scenario, in which two neutrino eigenstates are much heavier than the third one, and nearly degenerate. Cosmological observations are approaching this stringent upper bound, and will be able to impact neutrino science – in synergy with particle physics experiments. However, a main limitation from cosmology is the necessary model dependency, and the sensitivity only to kinematic properties but not on the actual particle content.

Several cosmological probes can be used to study massive neutrinos. The most direct route

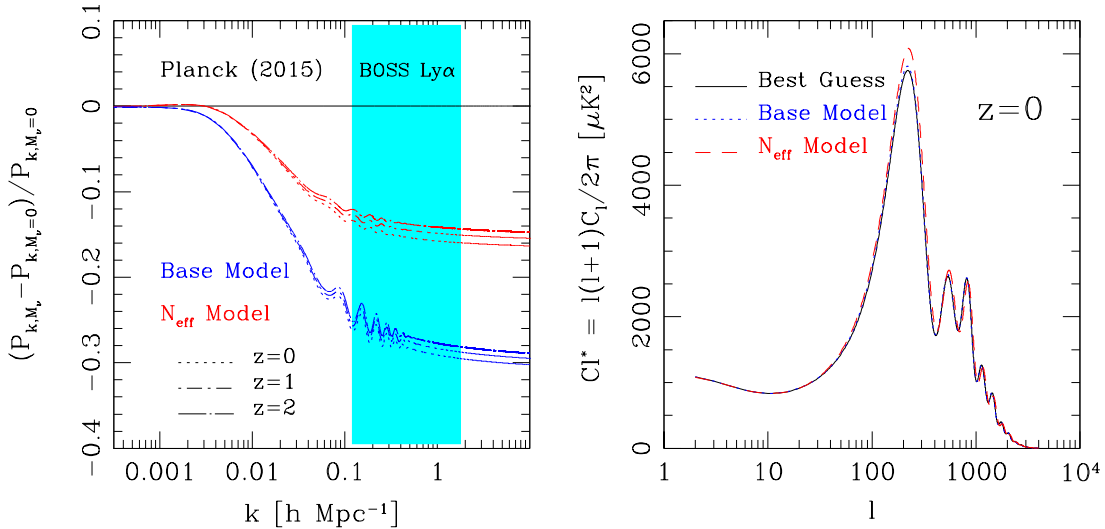


Figure 1 – [Left] Linear theory predictions for the total matter power spectra in a massive neutrino cosmology where $\sum m_\nu = 0.3$ eV (blue lines, ‘base model’) and in a non-standard model with a sterile neutrino so that $N_{\text{eff}} = 4.046$ eV (red lines, ‘ N_{eff} model’), normalized by the baseline Planck (2015) reference cosmology. See the text for more details. Different line styles show the evolution in redshift ($z = 0, 1, 2$), as a function of the total neutrino mass. The cyan zone highlights the k -range covered by the 1D flux power spectrum obtained from the Ly α BOSS survey. [Right] Corresponding CMB temperature power spectra for the same models.

is via the cosmic microwave background (CMB), particularly in polarization maps,^{12,13,14} but many other baryonic tracers of the LSS clustering of matter are also quite sensitive to neutrino properties. Examples include the 3D power spectrum from galaxy surveys, the Sunyaev-Zel’dovich effect in galaxy clusters, cosmic shear through weak lensing, or the Lyman- α (Ly α) forest.^{15,16,17,18} The latter observable is now re-emerging as a promising window into the high-redshift Universe; currently, the best Ly α forest data and the most precise measurement of the Ly α flux power spectrum come from the Baryon Acoustic Spectroscopic Survey (BOSS).¹⁰ In particular, the suppression of growth of cosmological structures on scales smaller than the neutrino free-streaming distance makes the Ly α forest a good tracer of the neutrino mass, and measurements of the mean Ly α transmission flux allow one to constrain the basic cosmological parameters with improved sensitivity. We will focus particularly on the Ly α forest in this study.

Because neutrinos are very light particles and weakly interacting, they free-stream over large distances erasing pre-existing structures and causing a characteristic suppression of power on small scales. This effect can be clearly seen in the linear matter power spectrum (P_{k,M_ν} versus $P_{k,M_\nu=0}$), as shown in Figure 1 where we consider two distinct massive neutrino cosmologies normalized by the standard Λ CDM Planck (2015) concordance model – which includes a minimal neutrino mass of 0.06 eV. Specifically, blue lines refer to the ‘base model’ with three degenerate massive neutrinos having a total mass $\sum m_\nu = 0.3$ eV and no massless neutrinos, while red lines refer to a non-standard ‘ N_{eff} model’ with three massive neutrinos of total mass 0.3 eV and an additional thermalized sterile neutrino, so that $N_{\text{eff}} = 4.046$. The latter model will be discussed more thoroughly in Section 5. Different line styles refer to different redshifts ($z = 0, 1, 2$), as indicated in the panels. Note the mass- and redshift-dependent suppression of power at small scales. All the various linear predictions are computed with the CAMB code.¹⁹ The cyan area in the left figure shows the k -range covered by the BOSS survey, relatively to the 1D Ly α forest power spectrum. The right panel shows corresponding CMB temperature power spectra for the same models. Note the small differences in the scale of BAO and CMB peaks: when we relate the two different cosmologies via our analytic remapping in Section 5, small differences in the CMB power spectra will still remain but they do not affect the Ly α likelihood.

2 Simulating Massive Neutrinos

Neutrinos are elusive particles, and therefore the neutrino implementation in numerical simulations is a non-trivial task. Neutrinos behave as extra radiation while ultra-relativistic, and as an additional cold dark matter (CDM) component when they become non-relativistic. The net result is a delay in matter domination.² Hence, they can be described either as a fluid or as an ensemble of particles, and treated within the context of linear theory or in a more complex fully non-linear regime. Neutrinos decouple from the cosmic plasma before the electron-positron annihilation (around ~ 1 MeV) resulting in a temperature T_ν lower than the photon temperature T_γ , and a number density n_ν lower than the photon number density. These effects can be parameterized by the fractional contribution to the matter density

$$f_\nu = \Omega_\nu/\Omega_m, \quad \Omega_\nu h^2 = \frac{\sum m_\nu}{93.14 \text{ eV}}, \quad (1)$$

where h is the present value of the Hubble constant in units of $100 \text{ km s}^{-1} \text{ Mpc}^{-1}$, and Ω_m is the matter energy density in terms of the critical density. Neutrinos in the mass range $0.05 \text{ eV} \leq m_\nu \leq 1.5 \text{ eV}$ become non-relativistic in the redshift interval $3000 \geq z \geq 100$, approximately around $z_{\text{nr}} \sim 2000 (m_\nu/1\text{eV})$ – during the matter domination era. When neutrinos are non-relativistic, there is a minimum wavenumber

$$k_{\text{nr}} \sim 0.018 \Omega_m^{1/2} \left[\frac{m_\nu}{1 \text{ eV}} \right]^{1/2} h/\text{Mpc} \quad (2)$$

above which the physical effect produced by their free-streaming damps small-scale density fluctuations, while modes with $k < k_{\text{nr}}$ evolve according to linear theory. Depending on the particular description adopted, one has to face different challenges. In particular, due to their high-thermal velocities, a severe limitation is posed by the presence of shot-noise.

Several roots have been followed in the literature to implement massive neutrinos numerically, ranging from linear theory approximations to hybrid approaches, fluid descriptions and grid methods, and particle implementations.^{20,21,22,23,24} For our simulations we choose a more direct approach: neutrinos are modeled as an additional type of particle in the N -body setup (on top of gas and CDM), and a full hydrodynamical treatment is carried out, well-inside the nonlinear regime – including the effects of baryonic physics which affect the intergalactic medium (IGM). The adopted implementation technique is driven by our goal to accurately reproduce all the main features of the Ly α forest, at the quality level of BOSS or future deep Ly α surveys.

Our simulations are produced using Gadget-3, a massively parallel tree-SPH code for collisionless and gasdynamical cosmological simulations modified in order to simulate the evolution of the neutrino density distribution.²⁵ Initial conditions are determined using the CAMB code, complemented by second-order Lagrangian perturbation theory (2LPT).^{19,26} Gravitational interactions are computed with a hierarchical multipole expansion via the standard N -body method, and gas-dynamics is followed with SPH having fully adaptive smoothing lengths, so that energy and entropy are conserved. Short-range forces are treated with the tree method, and long-range forces with Fourier techniques. Feedback options have been disabled, and galactic winds and the small-scale neutrino clustering are neglected.

A typical snapshot from Gadget-3 at a given redshift goes through an elaborate pipeline, in order to obtain an averaged flux power spectrum.²⁷ In particular, 100,000 randomly placed simulated quasar sightlines are drawn through the simulation box, and to generate the flux power spectrum the absorption due to each SPH particle near the sightline is calculated from the positions, velocities densities and temperatures of all the SPH particles at a given redshift.

For our study, we performed a large number of hydrodynamical simulations, both with varying neutrino mass and fixed cosmological and astrophysical parameters, or with a fixed neutrino mass and slight variations in the basic cosmological and astrophysical parameters around the reference cosmology. All our runs started at $z = 30$, with the gas assumed to be of primordial

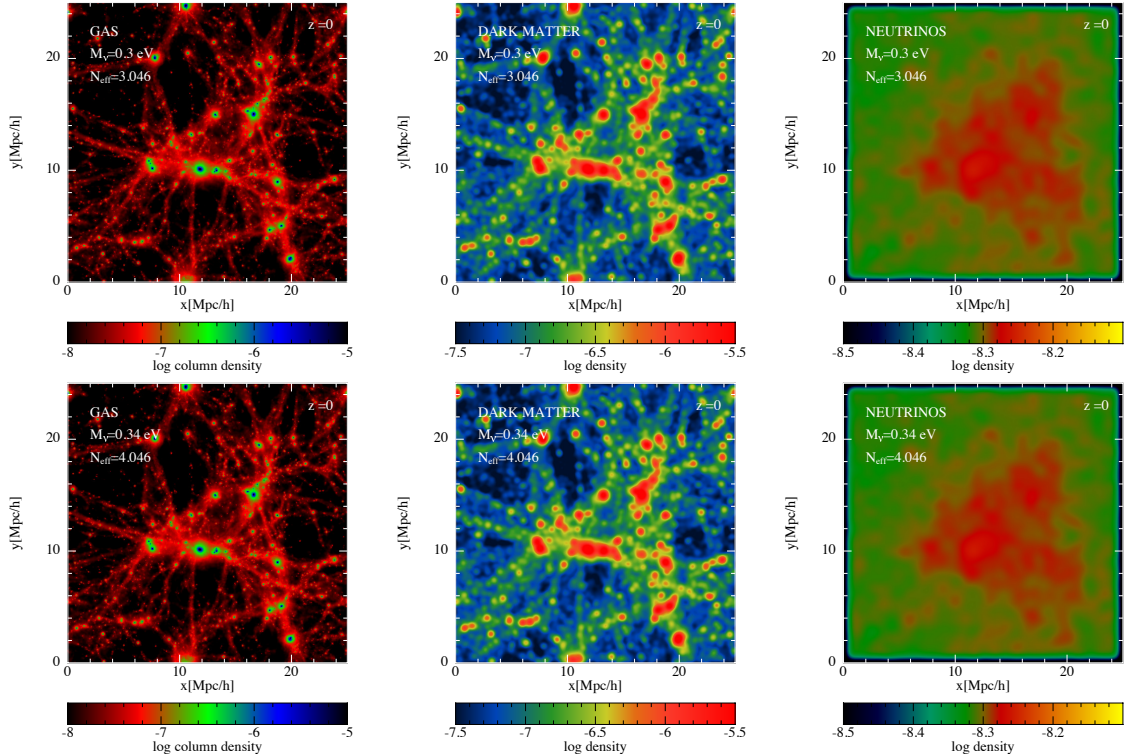


Figure 2 – Snapshots at $z = 0$ of the gas (left), dark matter (middle), and neutrino (right) densities, from simulations with $25h^{-1}\text{Mpc}$ box size and resolution $N_p = 192^3$ particles/type. Both standard (top panels, $N_{\text{eff}} = 3.046$) and non-standard (bottom panels, $N_{\text{eff}} = 4.046$) cosmologies are considered, for different values of the neutrino mass – related by the analytic remapping explained in Section 5.

composition (helium mass fraction of $Y = 0.24$), photo-ionised and heated by a spatially uniform ionising background, and neglecting metals and the evolution of elementary abundances. The various simulations were performed with periodic boundary conditions and an equal number of dark matter, gas, and neutrino particles. Snapshots are produced at regular intervals in redshift between $z = 4.6 - 2.2$, with $\Delta z = 0.2$. We also considered non-standard cosmologies where N_{eff} is different from the canonical value. For a given neutrino mass, we performed a set of three simulations with different box sizes and number of particles; specifically, we adopted a box size of $100 h^{-1}\text{Mpc}$ for large-scale power with a number of particles per component $N_p = 768^3$, and a box size of $25 h^{-1}\text{Mpc}$ for small-scale power, in this case with $N_p = 768^3$ or 192^3 , respectively. With a splicing technique,²⁸ we achieved an equivalent resolution of $3 \times 3072^3 \simeq 87$ billion particles in a $(100 h^{-1}\text{Mpc})^3$ box size – optimal also for eBOSS and DESI. When we included massive neutrinos we always kept $\Omega_\Lambda + \Omega_m$ fixed to give a flat geometry (with $\Omega_m = \Omega_b + \Omega_\nu + \Omega_{\text{CDM}}$) and vary the additional massive neutrino component Ω_ν to the detriment of Ω_{CDM} .

We provide a visual example of our snapshot outputs at $z = 0$ in Figure 2, for the gas (left panels), dark matter (central panels), and neutrino (right panels) components. The upper top panels are projections of the density field along the x and y directions (and across z) from a model with three degenerate massive neutrinos of total mass $\sum m_\nu = 0.3 \text{ eV}$ and no massless neutrinos, while the bottom panels refer to a non-standard cosmology with $N_{\text{eff}} = 4.046$, three degenerate massive neutrinos and a massless thermalized sterile neutrino. The relation between the two models is explained in Section 5. For all the simulations, the box size is $25 \text{ Mpc}/h$ and the resolution simply $N_p = 192^3$ particles per type. The axis scales are in Mpc/h . The various plots are smoothed with a cubic spline kernel.

3 Datasets

The datasets considered in this study consist of a combination of LSS and CMB probes. As LSS probes, we used the one-dimensional Ly α forest flux power spectrum derived from the Data Release 9 (DR9) of the BOSS quasar data,²⁹ combined with the measurement of the BAO scale in the clustering of galaxies from the BOSS Data Release 11 (DR11).³⁰ Specifically for the Ly α forest, our data consist of 13 821 quasar spectra, carefully selected according to their high quality, signal-to-noise ratio and spectral resolution, to bring systematic uncertainties at the same level of the statistical uncertainties. The Ly α forest flux power spectrum is measured in twelve redshifts bins, from $\langle z \rangle = 2.2$ to 4.4, in intervals of $\Delta z = 0.2$, and spans thirty-five wave numbers in the k range $[0.001 - 0.02]$, with k expressed in $(\text{km/s})^{-1}$. Correlations between different redshift bins were neglected, and the Ly α forest region was divided into up to three distinct z -sectors to minimize their impact. Noise, spectrograph resolution, metal contaminations and other systematic uncertainties were carefully subtracted out or accounted for in the modeling. As CMB probes, we adopted a combination of datasets collectively termed ‘CMB’, which includes Planck (2013) or (2015) temperature data (both high- ℓ and low- ℓ)^{31,14}, the high- ℓ public likelihoods from the Atacama Cosmology Telescope (ACT)³² and the South Pole Telescope (SPT)³³ experiments, and some low- ℓ WMAP polarization data.³⁴

4 Neutrino Mass Limits

To obtain constraints on neutrino masses and exploit the full information contained in the Ly α forest, we adopted a sophisticated technique based on the numerical simulations previously presented. Our central goal is to construct a multidimensional likelihood \mathcal{L} , as the product of individual likelihoods defining different cosmological probes (LSS and CMB), i.e., $\mathcal{L} = \mathcal{L}^{\text{LSS}} \mathcal{L}^{\text{CMB}} = \mathcal{L}^{\text{Ly}\alpha} \mathcal{L}^{\text{BAO}} \mathcal{L}^{\text{Planck}} \mathcal{L}^{\text{ACT}} \mathcal{L}^{\text{SPT}} \mathcal{L}^{\text{WMAP}}$. While \mathcal{L}^{CMB} and \mathcal{L}^{BAO} are directly taken from the corresponding experiments, we construct the Ly α forest likelihood with an elaborated procedure briefly described as follows. For a model \mathcal{M} defined by three categories of parameters – cosmological (α), astrophysical (β), nuisance (γ) – globally indicated with the multidimensional vector $\Theta = (\alpha, \beta, \gamma)$, and for a $N_k \times N_z$ dataset \mathbf{X} of power spectra $P(k_i, z_j)$ measured in N_k bins in k and N_z bins in redshift with experimental Gaussian errors $\sigma_{i,j}$, with $\sigma = \{\sigma_{i,j}\}$, $i = 1, N_k$ and $j = 1, N_z$, the Ly α likelihood is written as:

$$\mathcal{L}^{\text{Ly}\alpha}(\mathbf{X}, \sigma | \Theta) = \frac{\exp[-(\Delta^T C^{-1} \Delta)/2]}{(2\pi)^{\frac{N_k N_z}{2}} \sqrt{|C|}} \mathcal{L}_{\text{prior}}^{\text{Ly}\alpha}(\gamma) \quad (3)$$

where Δ is a $N_k \times N_z$ matrix with elements $\Delta(k_i, z_j) = P(k_i, z_j) - P^{\text{th}}(k_i, z_j)$, $P^{\text{th}}(k_i, z_j)$ is the predicted theoretical value of the power spectrum for the bin k_i and redshift z_j given the parameters (α, β) and computed from simulations, C is the sum of the data and simulation covariance matrices, and $\mathcal{L}_{\text{prior}}^{\text{Ly}\alpha}(\gamma)$ accounts for the nuisance parameters, a subset of the parameters Θ . For the fiducial model, we considered five cosmological parameters α in the context of the Λ CDM paradigm assuming flatness, i.e. $\alpha = (n_s, \sigma_8, \Omega_m, H_0, \sum m_\nu)$, four astrophysical parameters β related to the state of the IGM – two for the effective optical depth of the gas assuming a power law evolution, and two related to the heating rate of the IGM – and 12 nuisance parameters γ to account for imperfections in the measurements and in the modeling, plus two additional parameters for the correlated absorption of Ly α and either Si-III or Si-II. The theoretical Ly α power spectrum $P^{\text{th}}(k_i, z_j)$, as a function of α and β , is obtained via a second-order Taylor expansion around a central model chosen to be in agreement with Planck cosmological results, and computed using the grid of simulations described in Section 2. The global likelihood \mathcal{L} is finally interpreted in the context of the frequentist or bayesian approach.

Using this technique, we obtained $\sum m_\nu < 0.15$ eV at 95% CL for the combination Ly α +CMB, and $\sum m_\nu < 0.14$ eV at 95% when we further added BAO results when considering Planck

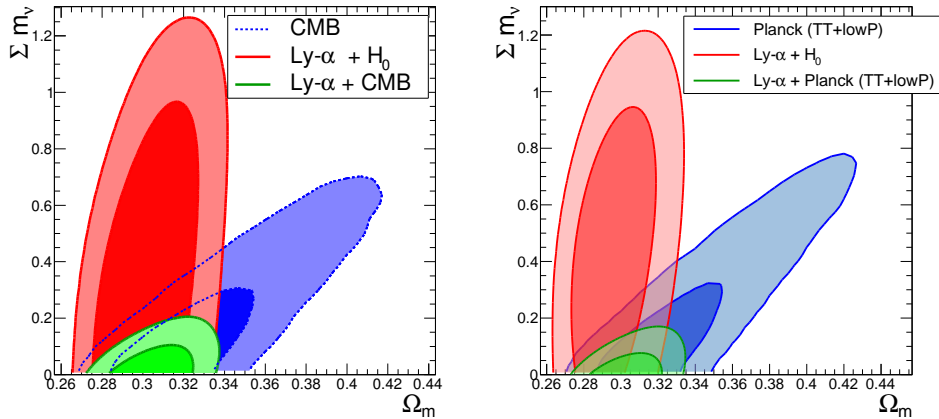


Figure 3 – 2D confidence level contours for Ω_m and $\sum m_\nu$ from a frequentist interpretation. The 68% and 95% confidence contours are obtained with different combinations of the BOSS Ly α and CMB data, as discussed in the main text. Planck (2013) data is used in the left panel, while the right panel is obtained with Planck (2015) data – resulting in a tighter upper bound on $\sum m_\nu$. Plots from Palanque-Delabrouille et al. (2015a,b).

(2013) data.⁶ We then improved our previous analysis and used Planck (2015) data, and obtained $\sum m_\nu < 0.12$ eV at 95% CL.⁷ Figure 3 highlights 2D confidence level contours for the $(\Omega_m, \sum m_\nu)$ cosmological parameters with a frequentist interpretation. In the left panel Planck (2013) data are considered, while in the right panel Planck (2015) data are adopted – reflecting in a tighter upper bound on the total neutrino mass. Ultimately, the sensitivity of cosmology in determining neutrino properties relies on the fact that neutrinos leave a redshift- and scale-dependent signature in the total matter power spectrum (see Figure 1, up to a 5% suppression of small-scale power) and in the galaxy distribution. Also, when combining different cosmological tracers with independent systematics the parameter space is significantly constrained – so that several parameter degeneracies can be lifted.

5 Number of Effective Neutrino Species

To include non-standard dark radiation scenarios in $\mathcal{L}^{\text{Ly}\alpha}$, we extended the parameter space Θ to account for models with sterile neutrinos or more generic relic radiation, where N_{eff} is different from the reference value (i.e. $N_{\text{eff}} = 3.046$). The Taylor expansion of the 1D Ly α flux power spectrum will then include further terms, but the logic leading to the construction of $\mathcal{L}^{\text{Ly}\alpha}$ is similar. Hence, in principle we just require additional cosmological hydrodynamical simulations to map out the extended parameter space and evaluate extra cross-derivative terms in the Taylor expansion. We avoided this computationally expensive procedure with a remapping strategy,⁸ based on the fact that if two even radically different cosmological models are characterized by the same linear matter power spectrum, they will also have nearly identical nonlinear matter and flux power spectra. Hence, one can simply rely on linear theory and on simulations with standard N_{eff} to specify more exotic dark radiation scenarios (see the test presented in the left panel of Figure 4). In practice, there should also be a small effect due to the fact that the expansion rate changes with N_{eff} , but this effect is ignored here since we neglect radiation density in our simulations.

By applying our extended technique we finally obtained $N_{\text{eff}} = 2.91_{-0.22}^{+0.21}$ (95% CL) and $\sum m_\nu < 0.15$ eV (95% CL) when we considered the combination CMB+Ly α , and $N_{\text{eff}} = 2.88 \pm 0.20$ (95% CL) and $\sum m_\nu < 0.14$ eV (95% CL) when we also added BAO information.⁸ This is shown in the right panel of Figure 4. Based on these assumptions, the main conclusions of our analysis are as follows: (1) the possibility of a sterile neutrino thermalized with active neutrinos – or more generally of any decoupled relativistic relic with $\Delta N_{\text{eff}} \simeq 1$ – is ruled out at

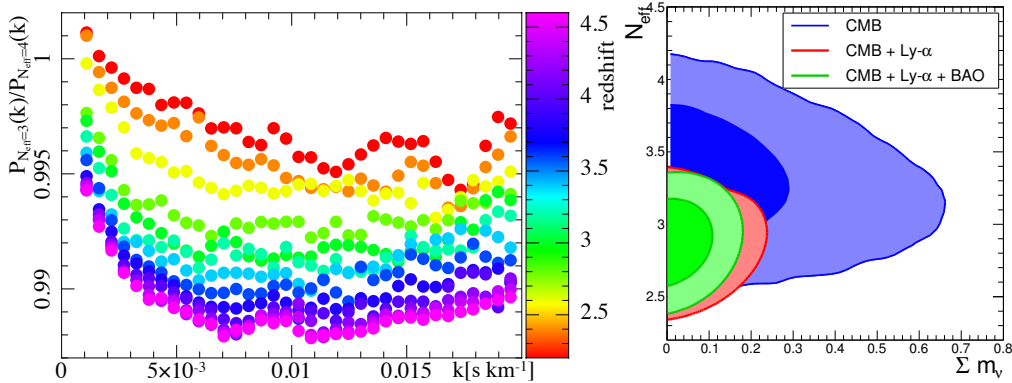


Figure 4 – [Left] Ratios of synthetic 1D Ly α flux power spectra extracted from a baseline model having three degenerate massive neutrinos and no extra relativistic degrees of freedom ($N_{\text{eff}} = 3$, $M_\nu = 0.35$ eV), and from a non-standard dark radiation model characterized by a massless sterile neutrino and three active neutrinos of degenerate mass. The cosmological parameters of the two models are fixed according to our remapping technique. At any given redshift, indicated by different colors in the figure, deviations in the corresponding power spectra are all within 1% (comparable to those obtained from linear theory), validating our analytic remapping also in the nonlinear regime. [Right] Joint constraints on N_{eff} and $\sum m_\nu$ from cosmological probes, as specified in the panel with different colors. In particular, our results exclude a sterile neutrino thermalized with active neutrinos at a significance of over 5σ (Rossi et al. 2015).

a significance of over 5σ , fully consistent with the latest constraints recently reported by Planck (2015); (2) we obtained a stringent upper bound on the total neutrino mass; (3) by rejecting $N_{\text{eff}} = 0$ at more than 14σ , our constraints provide strong evidence for the cosmic neutrino background (CNB) from $N_{\text{eff}} \sim 3$.

6 Particle Physics Synergies and Future Prospects

Cosmology is becoming progressively competitive in constraining the properties of massive neutrinos, in synergy with particle physics experiments. To this end, a multidisciplinary approach in neutrino science is essential. In fact, our results have several implications for particle physics experiments, as discussed in our recent publications.^{6,7,8,35} For example, our stringent upper bounds on $\sum m_\nu$ suggest interesting complementarity with future particle physics direct measurements of the effective electron neutrino mass,³⁶ and for neutrinoless double beta decay experiments.³⁷

In our work, we have presented a new technique to constrain neutrino masses and the number of effective neutrino species, in particular using the Ly α forest as a high- z tracer. We have obtained stringent upper bounds on the total neutrino mass (up to $\sum m_\nu < 0.12$ eV at 95% CL), and a tight constraint on N_{eff} ($N_{\text{eff}} = 2.88 \pm 0.20$ at 95% CL). Our results tend to favor the normal hierarchy for the total neutrino mass, exclude a sterile neutrino thermalized with active neutrinos at more than 5σ , and provide convincing evidence for the CNB from $N_{\text{eff}} \sim 3$ ($N_{\text{eff}} = 0$ is rejected at more than 14σ). Large-volume cosmological surveys such as DESI, 4MOST, or Euclid are expected to provide tightest constraints on neutrinos and eventually solve the hierarchy problem, although already with the SDSS-IV eBOSS it may be possible to distinguish between the two scenarios of neutrino mass hierarchies.³⁸ For N_{eff} the situation is more complicated, and likely major improvements will come from Stage-IV CMB experiments.

Acknowledgments

This work and the participation to the ‘Rencontres de Moriond’ (March 2016) in La Thuile, Aosta Valley, Italy, were supported by the National Research Foundation of Korea (NRF) through NRF-SGER 2014055950 funded by the Korean Ministry of Education, Science and Technology (MoEST), and by the faculty research fund of Sejong University in 2016. Some numerical

simulations presented in this work were performed using the Korea Institute of Science and Technology Information (KISTI) supercomputing infrastructure under allocation KSC-2016-G2-0004. It is a pleasure to thank Jacques Dumarchez for the superb organization, along with the scientific and organizing committees and the secretariat. Many congratulations for the 50th Moriond anniversary!

References

1. Mangano, G., Miele, G., Pastor, S., et al. 2005, Nuclear Physics B, 729, 221
2. Lesgourgues, J., & Pastor, S. 2006, Phys. Rep., 429, 307
3. Beringer, J., Arguin, J.-F., Barnett, R. M., et al. 2012, Phys. Rev. D, 86, 010001
4. Seljak, U., Slosar, A., & McDonald, P. 2006, *JCAP*, 10, 14
5. Riemer-Sørensen, S., Parkinson, D., Davis, T. M., & Blake, C. 2013, ApJ, 763, 89
6. Palanque-Delabrouille, N., Yèche, C., Lesgourgues, J., et al. 2015, *JCAP*, 2, 045
7. Palanque-Delabrouille, N., Yèche, C., Baur, J., et al. 2015, *JCAP*, 11, 011
8. Rossi, G., Yèche, C., Palanque-Delabrouille, N., et al. 2015, Phys. Rev. D, 92, 063505
9. Di Valentino, E., Giusarma, E., Lattanzi, M., et al. 2016, Physics Letters B, 752, 182
10. Dawson, K. S., Schlegel, D. J., Ahn, C. P., et al. 2013, AJ, 145, 10
11. Levi, M., Bebek, C., Beers, T., et al. 2013, arXiv:1308.0847
12. Hinshaw, G., Larson, D., Komatsu, E., et al. 2013, ApJS, 208, 19
13. Planck Collaboration, Ade, P. A. R., Aghanim, N., et al. 2014, A&A, 571, AA16
14. Planck Collaboration, Ade, P. A. R., Aghanim, N., et al. 2015, arXiv:1502.02114
15. Zaldarriaga, M., & Seljak, U. 1998, Phys. Rev. D, 58, 023003
16. Abazajian, K., & Dodelson, S. 2003, Physical Review Letters, 91, 041301
17. Santos, L., Cabella, P., Balbi, A., & Vittorio, N. 2013, Phys. Rev. D, 88, 043505
18. Battye, R. A., Moss, A., & Pearson, J. A. 2015, *JCAP*, 4, 048
19. Lewis, A., Challinor, A., & Lasenby, A. 2000, ApJ, 538, 473
20. White, S. D. M., Frenk, C. S., & Davis, M. 1983, ApJ, 274, L1
21. Ma, C.-P., & Bertschinger, E. 1994, ApJ, 429, 22
22. Brandbyge, J., & Hannestad, S. 2010, *JCAP*, 1, 21
23. Ali-Haïmoud, Y., & Bird, S. 2013, MNRAS, 428, 3375
24. Villaescusa-Navarro, F., Bird, S., Peña-Garay, C., & Viel, M. 2013, *JCAP*, 3, 19
25. Springel, V., Yoshida, N., & White, S. D. M. 2001, New Astronomy, 6, 79
26. Crocce, M., Pueblas, S., & Scoccimarro, R. 2006, MNRAS, 373, 369
27. Rossi, G., Palanque-Delabrouille, N., Borde, A., et al. 2014, A&A, 567, AA79
28. McDonald, P. 2003, ApJ, 585, 34
29. Palanque-Delabrouille, N., Yèche, C., Borde, A., et al. 2013, A&A, 559, A85
30. Anderson, L., Aubourg, É., Bailey, S., et al. 2014, MNRAS, 441, 2
31. Planck Collaboration, Ade, P. A. R., Aghanim, N., et al. 2014, A&A, 571, AA15
32. Das, S., Louis, T., Nolta, M. R., et al. 2014, *JCAP*, 4, 014
33. Reichardt, C. L., Shaw, L., Zahn, O., et al. 2012, ApJ, 755, 70
34. Bennett, C. L., Larson, D., Weiland, J. L., et al. 2013, ApJS, 208, 20
35. Rossi, G. 2015, Publication of Korean Astronomical Society, 30, 321
36. Capozzi, F., Fogli, G. L., Lisi, E., et al. 2014, Phys. Rev. D, 89, 093018
37. Dell’Oro, S., Maccioni, S., Viel, M., & Vissani, F. 2015, *JCAP*, 12, 023
38. Zhao, G.-B., Wang, Y., Ross, A. J., et al. 2016, MNRAS, 457, 2377